Original Article

Biosynthesis, characterization and evaluation of the supportive properties and biocompatibility of DBM nanoparticles on a tissue-engineered nerve conduit from decellularized sciatic nerve

Faezeh Nasrollahi nia [a], Asadollah Asadi [a, *], Saber Zahri [a], Arash Abdolmaleki [b, c]

[a] Department of Biology, Faculty of Science, University of Mohaghegh Ardabili, Ardabil, Iran
[b] Department of Engineering Sciences, Faculty of Advanced Technologies, University of Mohaghegh Ardabili, Namin, Iran
[c] Bio Science and Biotechnology Researchcenter (BBRC), Sabalan University of Advanced Technologies (SUAT), Namin, Iran

ARTICLE INFO

ABSTRACT

In this study, we examined the supporting effects of nano-demineralized bone matrix on the cultivation of Wharton's jelly stem cells on acellularized nerve scaffold. Demineralized bone matrix nanoparticles were prepared and characterized by several experiments. Decellularized sciatic nerve scaffolds were prepared and their efficiency was evaluated using histological stainings and biomechanical testing. Results of histological staining indicated that the integrity of the extra cellular matrix components was preserved. Also, the growth and viability of WJSCs on the scaffolds were significantly higher in DBM nanoparticle groups. We conclude that supportive properties of nano-DBM groups showed better cell viability and a suitable microenvironment for proliferation, retention, and adhesion of cells compared with other groups.

1. Introduction

Regenerative medicine is wide field of medical sciences in which some types of cells, broadly stem cells, are used to reconstruct injured tissues or organs. The ultimate goal of regenerative medicine is to establish and restore normal functions of organs [1,2]. Tissue engineers continue to develop innovative material compositions and designs from synthetic to natural materials with physical, chemical, and biological properties similar to the target tissues. This provides many alternatives to optimally regenerate or construct neo-tissues and neo-organs [3]. The selection of biomaterials is the first step in the construction of scaffolds with high efficiency for supporting the proliferation and differentiation of cells [4,5]. Following severe peripheral nerve injury, the current clinical gold standard for repair of nerve transection is the nerve autograft [6,7]. But the use of autografts has some limitations, such as the availability of donor nerves, donor site morbidity, and mismatch in size between the donor and recipient nerves [8,9].

Mesenchymal stem cells (MSCs) can be isolated from various sources and expanded easily *in vitro* [10,11]. Recently umbilical cord Wharton's jelly has been recognized as an excellent source for the isolation of MSCs by researchers because it contains fully characterized MSCs with high proliferation rates [12,13]. These cells have been shown to be hypoimmunogenic and secrete some growth factors [14]. Additionally, Wharton's jelly stem cells (WJSCs) can differentiate into different cell types [13]. Due to the unique characteristics of WJSCs, they have been considered by many researchers for therapeutic applications in regenerative medicine [14,15]. In this regards, the best alternative to a nerve autograft for clinical use is the combination of acellularized nerve scaffold (ANS) and stem cells [7].

Stem cells are be lost in the early hours after transplantation due to the harmful microenvironment of the injured site, where there is as ionic imbalance, oxidative stress, energy failure, neurotrophic factor deprivation, and apoptosis of the cells [16,17]. Low survival rate and retention of transplanted MSCs limits their therapeutic potential for regenerative medicine [18,19]. Therefore, any agents that attenuate the above-mentioned mechanisms may enhance the survival rate and retention of transplanted MSCs and can be used for the nerve regeneration process.

Demineralized bone matrix (DBM) is a cell matrix produced by acid demineralization of whole bone [20]. In the process of producing DBM, the soluble noncollagenous proteins are removed, while native insoluble bone morphogenetic proteins (BMPs), bone sialoprotein, transforming growth factor-β, Acidic fibroblast growth factor, vascular endothelial growth factor, and platelet-derived growth factor are retained. Previous studies have shown that DBM can induce the differentiation of MSCs into chondrocytes *in vitro* [20−23]. In addition to bone matrix proteins and the predominant protein − type I collagen, some notable protein pleiotropic growth factors are present and released from DBM [23].

The BMPs belong to the large family of transforming growth factors (TGF) and contribute to bioactivity [24]. They have an important role in the control of limb development, neural tube formation, neuronal survival, and apoptosis [25,26]. Other research has demonstrated that intracerebrally implanted MSCs delay the onset of neurological abnormalities of acid sphingomyelinase deficient mice and consequently prolong the life span of these mice [27]. Bone morphogenetic protein-2 (BMP-2) is a cytokine that can stimulate MSC proliferation and differentiation in rats [28]. In this study, we examined the supporting effects of nano-DBM on the cultivation of Wharton's jelly stem cells (WJSCs) on an acellularized nerve scaffold.

2. Materials and methods

2.1. Biosynthesis of DBM nanoparticles

To synthesize the DBM nanoparticles, demineralized bone matrix was prepared from fresh cow femurs. The bones were cut into blades using a scalpel and then freeze drying was used to dehydrate the scaffold, which was then converted into nano-powder using a Baloot Mill (NARYA-BM25, Iran).

2.2. Characterization of DBM nanoparticles

Following synthesis of the DBM nanoparticles, the nanoparticles were characterized through several experiments to confirm their size, shape, surface, and morphological features. The shape and surface morphology of the DBM nanoparticles was determined using atomic force microscopy (AFM). DBM nanoparticles were suspended in distilled water, then a drop of suspension was placed on the glass coverslip, air-dried, and scanned using AFM (Agilent 5500 AFM, USA). Also, the ultra-structural nature and morphological distinctiveness of DBM nanoparticles have been investigated and confirmed using field emission scanning electron microscopy (FESEM) Philips JSM- 6360LA instrument (Philips, Eindhoven, Netherlands).

2.3. Isolation, culture and identification of WJSCs

In the present study, human umbilical cords were collected following Cesarean with the consent of the mothers at the obstetrical department of Arta Hospital, Ardabil University of Medical Sciences, Ardabil, Iran. All experimental procedures were in accordance with the Nation Institutes of Health guide for the care and use of Laboratory animals (NIH Publications No. 8023, revised 1978). Also, in accordance with the guidelines of the Ethics Committee of the Mohaghegh Ardabili University of Ardabil (Iran).

Briefly, the cords were washed with 70% alcohol, then were sectioned into 2 cm pieces in Hanks balanced salt solution (HBSS), and blood vessels were separated from the Wharton's jelly. After this, Wharton's jelly was chopped into pieces of approximately 0.5 mm using a scalpel, then pieces were cultured in low glucose Dulbecco's modified Eagle's medium (DMEM, Gibco, Germany)

containing 20% fetal bovine serum (FBS, Gibco, Germany) and 1% Penstrep (Sigma, USA) in 75 cm^2 flasks (SPL, Korea) [29,30].

The cultures were maintained at 37 °C with 5% CO_2 and the culture was changed every 3 days. Cells of the third passage were used in our experiments. To confirm multipotency, passage 3 WJSCs were cultured in adipogenesis and osteogenesis differentiation media (Invitrogen, USA) according to the manufacturer's protocol. The culture was changed every 3 days. After 3 weeks of culture, the WJSCs were subjected to Oil Red O staining for adipogenesis and with Alizarin Red for matrix mineralization of osteogenesis. To confirm WJSCs phenotype, the cells at passage 3 were subjected to flow cytometry to determine the surface expression of CD29, CD90, CD105, CD34, and CD45 markers (BD Biosciences, USA), as described by the manufacturer. Cells stained with FITC-conjugated IgG1κ, IgA, and IgM were used as isotype controls. Flow cytometry was performed using a BD FACSCalibur flow cytometer (BD Biosciences) and analysis was performed using FlowJo v 10 (TreeStar) software. All cells in the experiment were third passage.

2.4. Acellular nerve allograft (ANA) preparation

Adult male Wistar rats (200−250 g) were sacrificed through an i.p. injection with sodium pentobarbital. Then sciatic nerves were excised and decellularized as previously described by Sondell [31]. Briefly, sciatic nerves were agitated in tubes filled with deionized distilled water for 7 h. Then, water was aspirated and nerve tissues were exposed to 3% Triton X-100 (Sigma) in distilled water for 12h, after which the water was replaced with a solution containing 4% sodium deoxycholate (Sigma) for 24 h. These steps were repeated again and, after a final wash with distilled water, the prepared ANA were stored in PBS buffer solution (pH 7.4) containing penicillin and streptomycin at 4 °C until use.

2.5. Histological evaluation of ANA

Histological analyses were used to evaluate the surface morphology of the basement membrane and extra cellular matrix (ECM) components after decellularization. Intact nerve and ANA histological sections were stained with hematoxylin and eosin (H&E) to observe general morphology. In brief, the tissue specimens were fixed using 10% formalin. Next, dehydration was performed with graded, increasing ethanol concentrations and then xylene. Samples were paraffin-embedded, and transverse sections with a thickness of 5 μm were prepared. Tissue sections were deparaffinized by xylene and rehydrated with graded, decreasing ethanol concentrations. The sections were then stained with H&E according to standard procedures, and prepared slides were observed under a light microscopy (Olympus, Japan).

To confirm that collagen fibers remained, prepared sections of ANA and intact nerve were stained with van Gieson's picro-fuchsin as described previously [32]. Also, to confirm cell elimination and to check the residual DNA in samples, prepared sections of ANA were stained with 4′,6-Diamidino-2-phenylindole (DAPI; Merck) as described previously. In brief, prepared nerve sections were deparaffinized by xylene and rehydrated with graded, decreasing ethanol concentrations. Then, slides were drained and incubated with DAPI staining solution (200 μl) for 15 min in a dark place. Next, stained slides were observed and analyzed under a fluorescence microscope (Olympus, Japan).

2.6. Evaluation of biomechanical properties

Intact nerve and ANA specimens underwent biomechanical tests (n = 5/group). Specimens were loaded onto a Universal Testing Machine (SANTAM-STM20, Tehran, Iran). In brief,
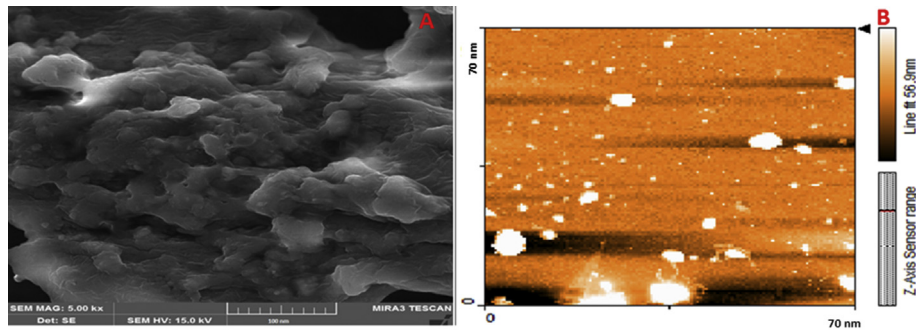
Fig. 1. FE-SEM images of DBM nanoparticles (A). AFM picture of DBM nanoparticles showing core—shell structure of nanoparticles. The nanoparticles were nearly spherical in shape (B).

specimens were placed between two grips of the tensile tester. Then, specimens were stretched at a strain rate of 0.05 mm/s until they were torn. The mean specimen length was 10 mm and samples were kept wet during experiments by applying PBS to the specimens. Intact sciatic nerves were used as controls.

2.7. Effects of Nano-DBM on WJSCs viability and proliferation in normal condition

The MTT assay was performed to evaluate WJSC viability and proliferation after culturing by measuring metabolic activity, under normal conditions. Afterwards, cells were subjected to the experimental treatments for 24 h. The cells were incubated with 20 μl MTT reagent (5 mg/ml; St. Louis, MO, USA) in the dark at 37 °C for 4 h. Following incubation, the medium was removed completely and formazan crystals were dissolved in 200 μl of dimethyl sulfoxide (DMSO; Sigma) for 1 h. The absorbance of each sample was measured at a wavelength of 570 nm using a microplate reader (model 550; Bio-Rad Laboratories, Hercules, CA, USA). Absorbance values correspond to the number of viable cells. Tissue culture polystyrene (TPS) was used as control. All experiments were conducted in triplicate.

2.8. Effects of Nano-DBM on WJSCs proliferation and retention on ANA

Evaluation of the effects of Nano-DBM on attachment, morphology, and retention of WJSCs on ANA was performed using MTT and SEM after 8 days of culture. In brief, 1×10^6 WJSCs were seeded onto each of the prepared ANA (5 mm) using a stereo microscope (Nikon, Japan). The cell—ANA combinations allowed attachment at 37 °C for 4 h. Then, the cell—ANA combinations were incubated on a 96-well plate containing (DMEM) with 10% FBS at 37 °C with 5% CO_2 for 8 days [33]. After that, the cell-ANA combinations were incubated with 20 μl MTT reagent (5 mg/ml; St. Louis, MO, USA) in the dark at 37 °C for 4 h. Following incubation, the
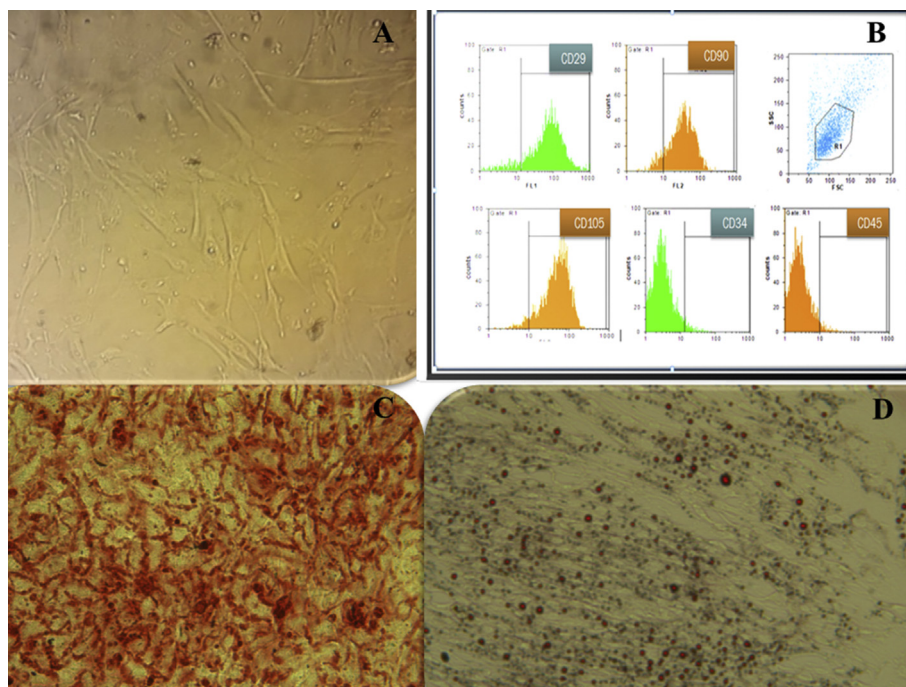

Fig. 2. Characteristics of mesenchymal cells from Wharton's jelly. (A): Wharton's jelly stem cells at passage 3. The cells have a fibroblast-like morphology. (B): Flow cytometric analysis of surface-marker expression on Wharton's jelly stem cells. The cells were cultured in Dulbecco's modified Eagle's medium supplemented with 10% fetal bovine serum. At passage 3, the cells were analyzed by flow cytometry. (C): Osteogenic differentiation potential of Wharton's jelly stem cells. Calcium crystals are shown in differentiated Wharton's jelly stem cells by alizarin red staining. (D): Adipogenic differentiation potential of Wharton's jelly stem cells. Lipid droplets are present in differentiated Wharton's jelly stem cells and stained red by oil-red-O staining.
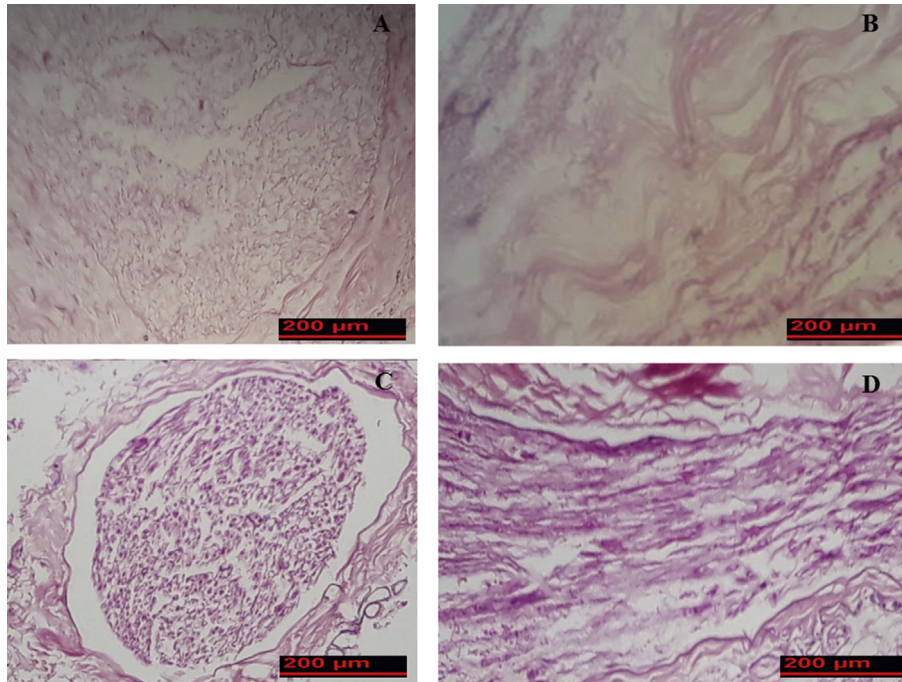
Fig. 3. General morphology of fresh rat sciatic nerve and acellular nerve allograft segments stained with hematoxylin and eosin. (A and C) Cross sections of acellular nerve and intact nerve respectively. (B and D) Longitudinal sections of acellular nerve and intact nerve respectively.

medium was removed completely and formazan crystals were dissolved in 200 μl of dimethyl sulfoxide (DMSO; Sigma) for 1 h. The absorbance of each sample was measured at a wavelength of 570 nm using a microplate reader (model 550; Bio-Rad Laboratories, Hercules, CA, USA). Tissue culture polystyrene (TPS) and untreated ANA were used as controls. After co-culturing for 8 days, the cell−ANA combinations were fixed with 4% glutaraldehyde for 12 h at 4 °C, samples were dehydrated by immersing in a gradual, increasing concentration of ethanol (up to 100%). Then, the samples were immersed in 100% acetone and coated with gold. Afterward, they were photographed with scanning electronic microscopy and cell attachment was measured using SEM micrographs.

2.9. Statistical analysis

Data analysis was performed using SPSS Statistics 16.0 software (SPSS Inc., Chicago, Illinois, USA). Statistical analysis was carried out using a one-way analysis of variance (ANOVA) to determine significant differences among the seven groups. Intergroup comparison of means was performed using a Tukey-Post hoc analysis. All data are expressed as mean ± standard error of the mean (SEM). Values of $P < 0.05$ were considered statistically significant.

3. Results

3.1. Nano-DBM characterization

FESEM is mainly employed as a new, important technique to evaluate the size distribution and morphology of particles. The FESEM images are shown in Fig. 1A. The results demonstrated that DBM nanoparticles are almost the same in size and nearly spherical in shape. The diameter of DBM nanoparticles was approximately 40−50 nm. Also, the AFM results confirmed that the surface and morphological features of nanoparticles showing round morphology and spherical shape (Fig. 1 B).
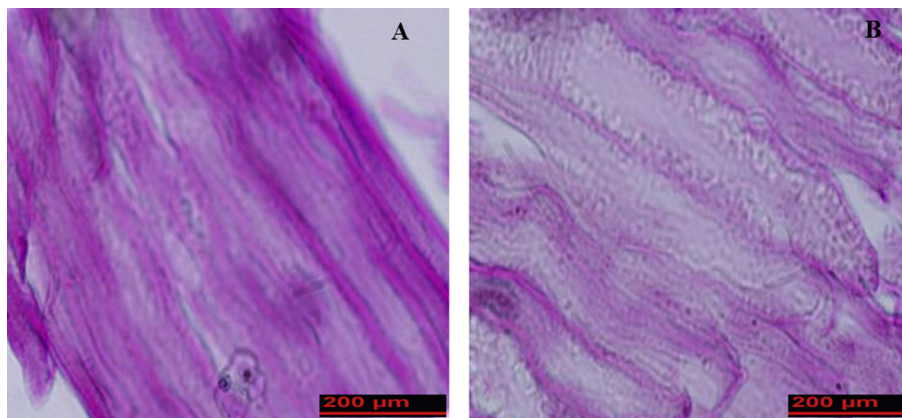

Fig. 4. Comparison of extracellular matrix preservation in intact nerve (A) and acellular nerve (B). Results of Van Gieson staining showed that structural components of the nerve (collagen and elastin fibers) were conserved.
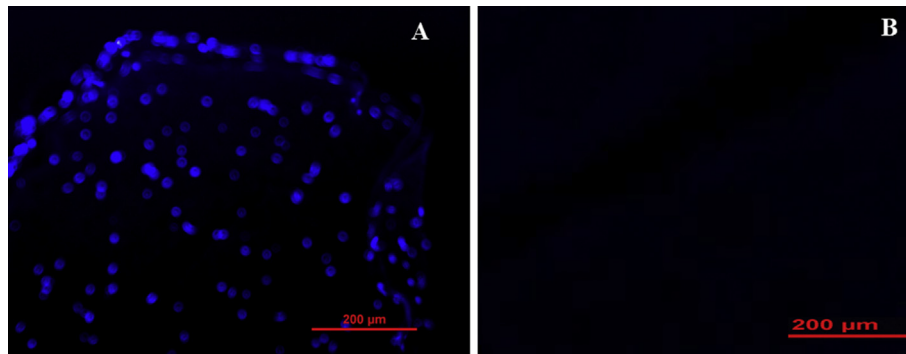
Fig. 5. DAPI-stained cross sections of rat sciatic nerve were used to compare the cell's nucleuses of freshly dissected nerve (A) and decellularized nerve segment (B). Results showed that the cell nucleuses had disappeared in decellularized nerve.

Table 1
Comparison of biomechanical properties of fresh nerve and acellular nerve scaffold (n = 5).

Groups	Peak Force (N)	Ultimate stress (MPa)	Ultimate Strain (%)	Peak Extension (mm)	Break stress (MPa)
Control	1.85 ± 0.25	0.73 ± 0.16	41.23 ± 11.24	5.41 ± 1.49	0.07 ± 0.07
ANA	1.30 ± 0.22*	0.52 ± 0.31*	63.34 ± 12.2*	7.22 ± 1.36*	0.21 ± 0.11*

3.2. WJSCs characterization

Cell cultures of WJSCs at passage 3 have a fibroblast-like morphology under inverted phase microscopy (Fig. 2A). To confirm the WJSC characterization, an immunophenotype of cultured WJSCs at passage 3 was performed by FACS analysis of surface marker expression. Results showed that WJSCs expressed high levels of CD29 (85.47 ± 1.3%), CD90 (83.85 ± 0.67%), and CD105 (94.53 ± 0.81%), but were negative for hematopoietic lineage markers CD34 (3.83 ± 0.01%) and CD45 (3.53 ± 0.3%) (Fig. 2B). To determine whether WJSCs have multipotent potential, we extracted WJSCs and cultured them in osteogenic and adipogenic medium. In osteogenic medium, the mineralization of calcium was detected using Alizarin Red S staining (Fig. 2C). Following adipogenic differentiation, the accumulation of intracellular lipid vacuole accumulation was detected using Oil Red O staining (Fig. 2D).

3.3. Characterization of ANA

Results of the study showed that the color of ANA after dcellularization was white and transparent. The elasticity diameter and length of ANA was slightly decreased in comparison with fresh nerves. Results of H&E staining showed that decellularziation was complete and, therefore, axon, myelin sheath, and cell nuclei were not present in prepared ANA (Fig. 3A and B). Normal nerve exhibited intact axons and the myelin sheath was mesh-like with faint staining. Schwann cells could be seen as deep blue in the normal nerves (Fig. 3C and D).

Van Gieson staining demonstrated no distinct disruption in matrix structure following the decellularization method. Additionally, structural components of the nerve (collagen and elastin fibers) were conserved in prepared ANA (Fig. 4).

DAPI staining of specimens showed that cells were completely removed and no residual DNA could be observed in the ANA group compared with intact nerve (Fig. 5).
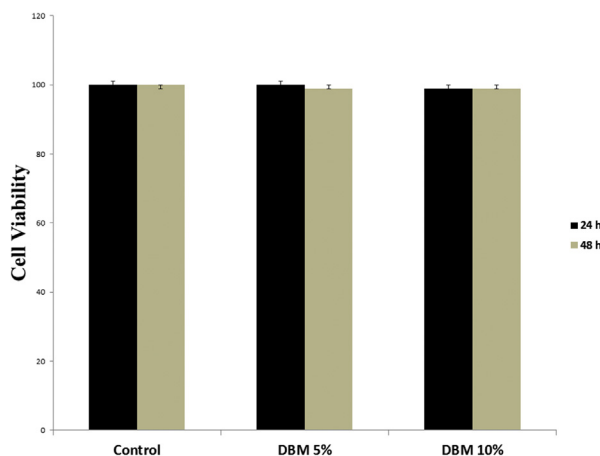

Fig. 6. Evaluation of Nano-DBM on WJSCs viability and proliferation under normal culture conditions. The viability and proliferation of seeded WJSCs in 96-well plates after 24 and 48 h using MTT assay shows that Nano-DBM had no toxic effect on cell viability and proliferation under normal culture conditions. The experiments were performed in triplicate (n = 10).
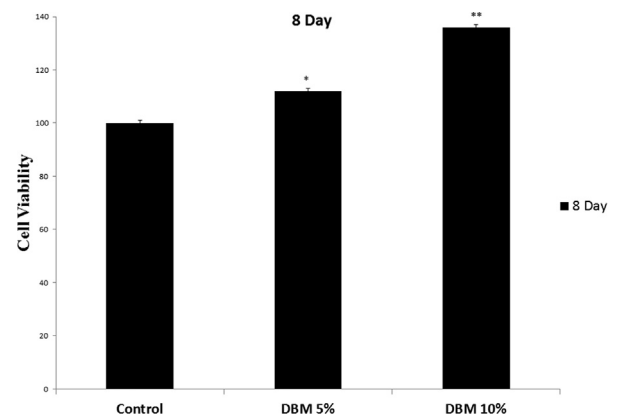

Fig. 7. Effects of Nano-DBM on biocompatibility and retention of WJSCs on ANA. The viability, proliferation, adhesion and maintenance of seeded WJSCs on ANA were investigated after 8 days of culture. Results indicated a significant increase in cell viability and proliferation in Nano-DBM treated groups compared to other groups (*P < 0.05, **P < 0.01). The experiments were performed in triplicate (n = 10).
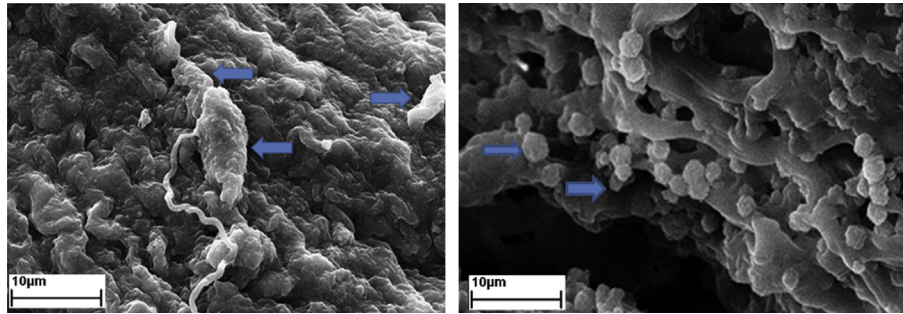
Fig. 8. Scanning electron micrographs showing that hWJSC (Arrows) are adhering to the ANA.

3.4. Tensile testing of ANA

The results of the biomechanical tests are shown in Table 1. Results indicated that there were no differences in the average lengths and widths of ANA in comparison with intact nerve and that there was no deterioration in ANA biomechanical properties. Additionally, tensile testing results showed that the mean ultimate stress, ultimate load, and breaking stress for ANA decreased significantly compared with the average for intact nerve (P < 0.05).

3.5. Effects of Nano-DBM on WJSCs viability and proliferation

To evaluate the effect of Nano-DBM on WJSCs viability, cells were treated with two different concentrations of Nano-DBM (5 and 10%) for 24 and 48 h under normal conditions. After culturing for 24 and 48 h, the colorimetric MTT assay result showed that Nano-DBM had no toxic effects on cultured WJSCs under normal conditions after culturing for 24 and 48 h (Fig. 6).

3.6. Effects of Nano-DBM on biocompatibility and retention of WJSCs on ANA

The adhesion and maintenance of seeded WJSCs at passage 3 on ANA were investigated after 8 days of culture. After culturing for 8 days, MTT assay results indicated a significant increase in cell viability and proliferation in Nano-DBM treated groups compared to other groups (*P < 0.05, **P < 0.01, Fig. 7). Moreover, the result indicated that ANA had no toxic effects on implanted WJSCs after culturing for 8 days. Scanning electron microscopy was used to evaluate the attachment and retention of WJSCs of ANA. SEM micrographs showed that cells adhered well to the ANA (Fig. 8). Also SEM micrographs showed that WJSCs were evenly distributed in the basilar membrane of ANA.

4. Discussion

The need to repair large defects in peripheral nerve is an important problem that neurosurgeons are faced with. Tissue engineering offers new strategies to enhance the utility of biomaterials for the development of new treatments [33,34].

Suitable scaffold is an essential needs for peripheral nerve tissue engineering as it provides a suitable microenvironment for cells proliferation and adhesion [35]. Also, it can secrete growth factors and promotes the axonal sprouts regeneration and nerve guides for accelerating axonal regeneration [36]. Tissue engineered scaffolds can provide conditions for better regeneration and increase the rate of vascularization in grafts [33,37]. Evaluating the decellularization protocol showed that all cellular components were removed successfully. Additionally, tissue architecture, ECM components, and biomechanical properties of the scaffolds were preserved. Although

removal of all cells and their components is necessary for preparing the tissue engineered scaffolds, retaining the ECM component intact is essential because it can promote the secretion of growth factors that provides suitable microenvironment for tissue remodeling, cell proliferation, and adhesion. Previous studies showed that ECM is more important in peripheral nerve regeneration because Schwann cells cannot form the Bungner band in the absence of basement membrane [38]. Results of tensile testing showed that ECM components like fibronectin, laminin, collagen, and elastin were preserved after decellularization. Damage to the basement membrane and ECM components such as collagen, fibronectin, and laminin can cause loss of the mechanical properties of tissue engineered scaffolds and decrease mechanical strength [39–41]. Based on checking the biomechanical properties of prepared scaffolds by evaluating their supportive properties, Nano-DBM groups showed better cell viability and a more suitable microenvironment for proliferation, retention, and adhesion of cells compared with other groups. Results showed that ECM provides a suitable microenvironment for cell adhesion and that Nano-DBM increased cell proliferation and viability on scaffold. Previous studies showed that tissue engineered scaffolds for peripheral nerve injuries should have biocompatibility and no antigenicity [42]. Previous studies have been shown that nanoparticle−cell interaction depends on surface aspects of scaffolds [43]. One practical characteristic of scaffolds for use in tissue engineering is cell adhesion [44]. SEM micrographs of our study showed that cells attached to each other and to scaffolds very well, and confirmed their attachments to the basement membrane.

In conclusion, the results showed that ECM of decellularized nerve scaffold provides a suitable microenvironment for cell adhesion and that Nano-DBM increased the cell viability, proliferation, and retention. Therefore, Nano-DBM can increase the effectiveness of scaffolds for peripheral nerve defects. It is clear that more research is needed to confirm these results.

Authors' contributions

Participated in research design: Asadi, Zahri, Abdolmaleki Conducted experiments: Nasrollahi, Abdolmaleki, Performed data analysis: Zahri, Asadi, Abdolmaleki, Wrote or contributed to the writing of the manuscript: Asadi, Zahri, Abdolmaleki, Nasrollahi.

Funding

The viability, proliferation, adhesion and maintenance of seeded WJSCs on ANA were investigated after 8 days of culture. Results indicated a significant increase in cell viability and proliferation in

Nano-DBM treated groups compared to other groups (*P < 0.05, **P < 0.01). The experiments were performed in triplicate (n = 10).

Declaration of Competing Interest

Authors declare that they have no conflict of interest.

Acknowledgments

References

[1] Orlando G, Wood KJ, Stratta RJ, Yoo JJ, Atala A, Soker S. Regenerative medicine and organ transplantation: past, present, and future. Transplantation 2011;91(12):1310e7.

[2] Iranpour S, Mahdavi-Shahri N, Miri R, Hasanzadeh H, Bidkhori HR, Naderi-Meshkin H, et al. Supportive properties of basement membrane layer of human amniotic membrane enable development of tissue engineering applications. Cell Tissue Bank 2018:1e15.

[3] Singh A, Lee D, Jeong H, Yu C, Li J, Fang CH, et al. Tissue-engineered neo-urinary conduit from decellularized trachea. Tissue Engineering Part A; 2018.

[4] Mano JF, Silva GA, Azevedo HS, Malafaya PB, Sousa RA, Silva SS, et al. Natural origin biodegradable systems in tissue engineering and regenerative medicine: present status and some moving trends. J R Soc Interface 2007;4(17):999e1030.

[5] Matsumine H, Sasaki R, Tabata Y, Matsui M, Yamato M, Okano T, et al. Facial nerve regeneration using basic fibroblast growth factor-impregnated gelatin microspheres in a rat model. J Tissue Eng Regenerat Med 2016;10(10):E559e67.

[6] Ghayour MB, Abdolmaleki A, Rassouli MB. Neuroprotective effect of Lovastatin on motor deficit induced by sciatic nerve crush in the rat. Eur J Pharmacol 2017;812:121–7.

[7] Ghayour M-B, Abdolmaleki A, Behnam-Rassouli M, Mahdavi-Shahri N, Moghimi A. Synergistic effects of ALCAR and adipose-derived stromal cells to improving regenerative capacity of acellular nerve allograft in sciatic nerve defect. J Pharmacol Exp Therapeut 2019;368(3):490–502.

[8] Neubauer D, Graham JB, Muir D. Nerve grafts with various sensory and motor fiber compositions are equally effective for the repair of a mixed nerve defect. Exp Neurol 2010;223(1):203–6.

[9] Mackinnon SE, Hudson AR. Clinical application of peripheral nerve transplantation. Plast Reconstr Surg 1992;90(4):695–9.

[10] Kern S, Eichler H, Stoeve J, Klüter H, Bieback K. Comparative analysis of mesenchymal stem cells from bone marrow, umbilical cord blood, or adipose tissue. Stem Cell 2006;24(5):1294e301.

[11] Deng J, Petersen BE, Steindler DA, Jorgensen ML, Laywell ED. Mesenchymal stem cells spontaneously express neural proteins in culture and are neurogenic after transplantation. Stem Cell 2006;24(4):1054e64.

[12] Baksh D, Song L, Tuan R. Adult mesenchymal stem cells: characterization, differentiation, and application in cell and gene therapy. J Cell Mol Med 2004;8(3):301–16.

[13] Khatami SM, Zahri S, Maleki M, Hamidi K. Stem cell isolation from human Wharton's jelly: a study of their differentiation ability into lens fiber cells. Cell J (Yakhteh) 2014;15(4):364.

[14] Fong CY, Gauthaman K, Cheyyatraivendran S, Lin HD, Biswas A, Bongso A. Human umbilical cord Wharton's jelly stem cells and its conditioned medium support hematopoietic stem cell expansion ex vivo. J Cell Biochem 2012;113(2):658e68.

[15] Fong CY, Subramanian A, Biswas A, Gauthaman K, Srikanth P, Hande MP, et al. Derivation efficiency, cell proliferation, freezeethaw survival, stem-cell properties and differentiation of human Wharton's jelly stem cells. Reprod Biomed Online 2010;21(3):391e401.

[16] Martinou J-C, Youle RJ. Mitochondria in apoptosis: bcl-2 family members and mitochondrial dynamics. Dev Cell 2011;21(1):92–101.

[17] Toma C, Pittenger MF, Cahill KS, Byrne BJ, Kessler PD. Human mesenchymal stem cells differentiate to a cardiomyocyte phenotype In the adult murine heart. Circulation 2002;105(1):93e8.

[18] Potier E, Ferreira E, Meunier A, Sedel L, Logeart-Avramoglou D, Petite H. Prolonged hypoxia concomitant with serum deprivation induces massive human mesenchymal stem cell death. Tissue Eng 2007;13(6):1325e31.

[19] Fujimaki H, Matsumine H, Osaki H, Ueta Y, Kamei W, Shimizu M, et al. Dedifferentiated fat cells in polyglycolic acid-collagen nerve conduits promote rat facial nerve regeneration. Regen Ther 2019;11:240e8.

[20] Li X, Jin L, Balian G, Laurencin CT, Anderson DG. Demineralized bone matrix gelatin as scaffold for osteochondral tissue engineering. Biomaterials 2006;27(11):2426e33.

[21] Iwata HI, Ono SA, Sato KE, Sato TO, Kawamura MO. Bone morphogenetic protein-induced muscle-and synoviumderived cartilage differentiation in vitro. Clin Orthop Relat Res 1993;296:295e300.

[22] Nogami HI, Oohira AT, Terashima YO, Urist MR. Ultrastructure of chondrogenetic interactions between bone matrix gelatin and mesenchymal cells. Clin Orthop Relat Res 1978;133:238e45.

[23] Holt DJ, Grainger DW. Demineralized bone matrix as a vehicle for delivering endogenous and exogenous therapeutics in bone repair. Adv Drug Deliv Rev 2012;64(12):1123–8.

[24] Katz JM, Nataraj C, Jaw R, Deigl E, Bursac P. Demineralized bone matrix as an osteoinductive biomaterial and in vitro predictors of its biological potential. J Biomed Mater Res Part B: Appl Biomater: An Offi J Soc Biomater 2009;89(1):127e34 [The Japanese Society for Biomaterials, and The Australian Society for Biomaterials and the Korean Society for Biomaterials].

[25] D'alessandro JS, Yetz-Aldape J, Wang EA. Bone morphogenetic proteins induce differentiation in astrocyte lineage cells. Growth Factors 1994;11(1):53–69.

[26] Mehler MF, Mabie PC, Zhang D, Kessler JA. Bone morphogenetic proteins in the nervous system. Trends Neurosci 1997;20(7):309e17.

[27] Jin HK, Carter JE, Huntley GW, Schuchman EH. Intracerebral transplantation of mesenchymal stem cells into acid sphingomyelinaseedeficient mice delays the onset of neurological abnormalities and extends their life span. J Clin Invest 2002;109(9):1183e91.

[28] Akino K, Mineta T, Fukui M, Fujii T, Akita S. Bone morphogenetic protein-2 regulates proliferation of human mesenchymal stem cells. Wound Repair Regen 2003;11(5):354e60.

[29] Pereira RC, Costa-Pinto AR, Frias AM, Neves NM, Azevedo HS, Reis RL. In vitro chondrogenic commitment of human Wharton's jelly stem cells by co-culture with human articular chondrocytes. J Tissue Eng Regen Med 2017;11(6):1876e87.

[30] Maleki M, Ghanbarvand F, Behvarz MR, Ejtemaei M, Ghadirkhomi E. Comparison of mesenchymal stem cell markers in multiple human adult stem cells. Int J Stem Cell 2014;7(2):118.

[31] Sondell M, Lundborg G, Kanje M. Regeneration of the rat sciatic nerve into allografts made acellular through chemical extraction. Brain Res 1998;795(1–2):44–54.

[32] Prentø P, Van Gieson's picrofuchsin. The staining mechanisms for collagen and cytoplasm, and an examination of the dye diffusion rate model of differential staining. Histochemistry 1993;99(2):163–74.

[33] Gao S, Zheng Y, Cai Q, Yao W, Wang J, Zhang P, et al. Comparison of morphology and biocompatibility of acellular nerve scaffolds processed by different chemical methods. J Mater Sci Mater Med 2014;25(5):1283e91.

[34] Mohammad-Bagher G. Synergistic effects of Acetyl-L-carnitine and adipose-derived stromal cells to improving regenerative capacity of acellular nerve allograft in sciatic nerve defect. ASPET; 2019.

[35] Lynam D, Bednark B, Peterson C, Welker D, Gao M, Sakamoto JS. Precision microchannel scaffolds for central and peripheral nervous system repair. J Mater Sci Mater Med 2011;22(9):2119.

[36] Crapo PM, Medberry CJ, Reing JE, Tottey S, van der Merwe Y, Jones KE, et al. Biologic scaffolds composed of central nervous system extracellular matrix. Biomaterials 2012;33(13):3539e47.

[37] Freytes DO, Rundell AE, Geest JV, Vorp DA, Webster TJ, Badylak SF. Analytically derived material properties of multilaminated extracellular matrix devices using the ball-burst test. Biomaterials 2005;26(27):5518e31.

[38] Donzelli R, Maiuri F, Piscopo GA, de Notaris M, Colella A, Divitiis E. Role of extracellular matrix components in facial nerve regeneration: an experimental study. Neurol Res 2006;28(8):794e801.

[39] Connelly JT, García AJ, Levenston ME. Inhibition of in vitro chondrogenesis in RGD-modified three-dimensional alginate gels. Biomaterials 2007;28(6):1071–83.

[40] Bank RA, Krikken M, Beekman B, Stoop R, Maroudas A, Lafebers FP, et al. A simplified measurement of degraded collagen in tissues: application in healthy, fibrillated and osteoarthritic cartilage. Matrix Biol 1997;16(5):233e43.

[41] Niknejad H, Peirovi H, Jorjani M, Ahmadiani A, Ghanavi J, Seifalian AM. Properties of the amniotic membrane for potential use in tissue engineering. Eur Cell Mater 2008;15:88e99.

[42] Steed MB, Mukhatyar V, Valmikinathan C, Bellamkonda RV. Advances in bioengineered conduits for peripheral nerve regeneration. Atlas Oral Maxillofac Surg Clin North America 2011;19(1):119e30.

[43] Gupta AK, Curtis AS. Surface modified superparamagnetic nanoparticles for drug delivery: interaction studies with human fibroblasts in culture. J Mater Sci Mater Med 2004;15(4):493–6.

[44] Gholipourmalekabadi M, Sameni M, Radenkovic D, Mozafari M, Mossahebi-Mohammadi M, Seifalian A. Decellularized human amniotic membrane:how viable is it as a delivery system for human adipose tissue-derived stromal cells? Cell Prolif 2016;49(1):115e21.